ChemComm

COMMUNICATION

View Article Online
View Journal | View Issue

Cite this: *Chem. Commun.*, 2021, 57, 10095

Received 25th May 2021,
Accepted 9th August 2021

DOI: 10.1039/d1cc02538d

rsc.li/chemcomm

From organotin hydrides to heteronuclear main group metal compounds: isolation of the first neutral bismuth/tin clusters†

Beate G. Steller, Michaela Flock and Roland C. Fischer *

From conversions of Ar_2SnH_2 (Ar = Tripp, Dipp; Tripp = 2,4,6-Triisopropylphenyl, Dipp = 2,6-Diisopropylphenyl), and a bismuth(III) amide, $Bi[N(SiMe_3)_2]_3$, we isolated the first representatives of mixed, uncharged Bi/Sn clusters, $Bi_8Sn_3Ar_6$. Along with unprecedented bicyclo[2.2.0]-hexanes, $(HAr_2Sn)_2Sn_2Bi_4$, these have been characterized by single crystal X-Ray diffraction, heteronuclear NMR, vibrational and UV-Vis spectroscopy. Quantum-chemical calculations were carried out in order to understand bonding within the isolated polyhedral compounds.

Owing to potential applications in nano- and materials chemistry, the last few decades have seen tremendous progress in the field of main group element cluster chemistry. Yet, the number of examples and structural variety for this compound class is strongly dependent on the group number. In contrast to gallium and aluminum clusters and besides phosphorus and germanium, polyhedral compounds of heavier group 14 and 15 elements are still rare despite the advances in the last years,[1–3] let alone the examples of polyhedral mixed element compounds.[4–8] Apart from a limited number of examples of polyhedral phosphorus/tin compounds,[9–13] examples of more metallic arsenic, antimony and bismuth homologues are even rarer.[14–17] As homo- as well as heteroelement bond formation in these cases is still limited to just a few strategies including stoichiometric fusion of respective elements, derivatization of Zintl ions and reductive salt elimination, these heavier representatives are dominated by anionic Zintl ion-type structures.[18–21] In the case of Bi/Sn systems thus far overall only the structures of nine polyanions have been crystallographically characterized including also trimetallic systems,[22–30] while a series of neutral, unsubstituted Bi/Sn clusters were studied in the gas phase.[31,32] We currently investigate metathesis reactions between organotin hydrides and main group element amides as an alternative strategy for cluster synthesis in contrast to the more commonly used reductive and salt metathesis reactions. Hydrostannolysis and -germolysis of organoelement(IV)-hydrides and -amides have proven very useful for the synthesis of respective (alternating) oligo- and polymers.[33–35]

As an initial result, we herein report the first example of an uncharged polyhedral Bi/Sn compound, $Bi_8Sn_3Ar_6$, from the conversion of Ar_2SnH_2 (Ar = Tripp, Dipp) and a bismuth(III) amide. Addition of $Bi[N(SiMe_3)_2]_3$ to a DME solution of $Tripp_2SnH_2$ led to a color change from initially colorless to shortly red eventually fading to reddish brown within a few minutes. As initially a propellane-type structure, $Bi_2Sn_3Tripp_6$ was targeted, a stoichiometric ratio of 3 : 2 ($Tripp_2SnH_2$: $Bi[N(SiMe_3)_2]_3$) was applied. Respective, purely tin containing [1.1.1]propellanes were accessed from organotin hydrides and tin(II) amides subjected to similar reaction conditions in as yet unpublished results. Slow solvent evaporation from these reactions led to crystallization of brownish red rods suitable for X-ray crystallography after 6 days. Single crystal X-ray diffraction revealed the formation of the mixed bismuth/tin cage $Bi_8Sn_3Tripp_6$ (**1**, 13% yield referred to $Tripp_2SnH_2$, 53% yield referred to $Bi[N(SiMe_3)_2]_3$). **1** constitutes the first uncharged, polyhedral bismuth/tin compound. Storage of the supernatant solutions at −30 °C gave greenish yellow crystals of *cyclo*-$(Tripp_2Sn)_3$ (**2**)[36,37] as the main byproduct next to $H–N(SiMe_3)_2$ identified by NMR spectroscopy of reaction solutions.

In addition, small amounts of bicyclo [2.2.0]compound $Bi_4Sn_4H_2Tripp_6$ (**3**), were isolated from concentrated reactions mixtures. (Scheme 1 and Fig. 1, 2) In ^1H NMR analysis of **1**, broad resonances were observed at *r.t.* with even more broadened signals at elevated temperatures (35 and 45 °C), while cooling to −10 °C eventually gave well-resolved spectra with non-equivalent signals for *ortho*-*i*Pr groups of the substituents. (See ESI†) **1** exhibits also a broad $^{119}Sn\{^1H\}$ NMR resonance at −925 ppm (FWHM = 1230 Hz), which lacks comparable data in literature where only shifts for terminal $R_3Sn–Bi$ groups are available.[38–40] Attempts to increase the yield in **1** by adjusting the stoichiometry to 3 : 8 failed as no product was obtained nor detected by NMR spectroscopy, *cf.* Scheme S1 in ESI.†

Institute of Inorganic Chemistry, Graz University of Technology, Stremayrgasse 9, Graz 8010, Austria. E-mail: roland.fischer@tugraz.at

† Electronic supplementary information (ESI) available. CCDC 2072047–2072052. For ESI and crystallographic data in CIF or other electronic format see DOI: 10.1039/d1cc02538d

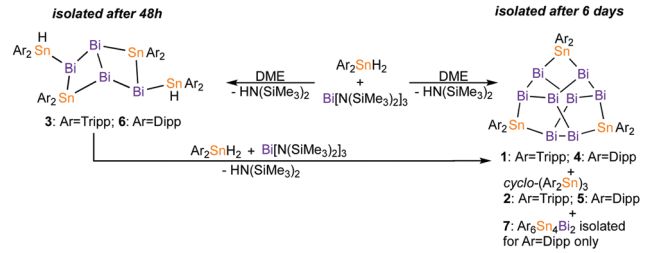

Scheme 1 Synthesis of $Bi_8Sn_3Ar_6$ (Ar = Tripp (**1**), Dipp (**4**)) from Ar_2SnH_2 and $Bi[N(SiMe_3)_2]_3$ in DME.

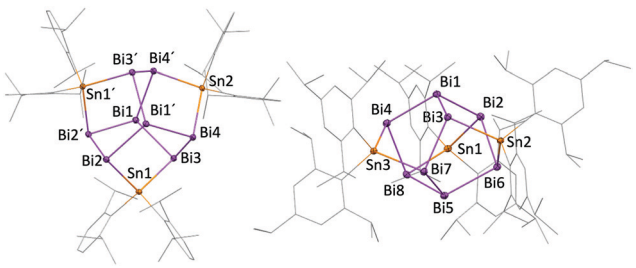

Fig. 1 Molecular structures of **1** (right) and **4** (left) in the solid state (50% probability), hydrogens are omitted. For key structural parameters *c.f.* Table 1.

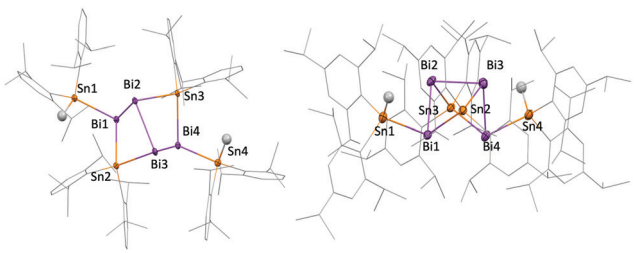

Fig. 2 Molecular structures (50% probability) of 6 (left) and 3 (right) in the solid state, hydrogens except Sn–H omitted.

When $Tripp_2SnH_2$ was replaced by the slightly less soluble dihydride $Dipp_2SnH_2$, slow concentration of the solvent after 2 days gave pale brownish red rhombic crystals suitable for X-ray crystallography which single crystal X-Ray diffraction revealed as the bicyclo [2.2.0]compound $Bi_4Sn_4H_2Dipp_6$ (**6**) in 4% yield. (Scheme 1 and Fig. 2). Nevertheless, evidence for the formation of the expected polyhedral $Bi_8Sn_3Dipp_6$, compound **4**, and *cyclo*-$(Dipp_2Sn)_3$ (**5**) were found in ^1H and ^{119}Sn NMR (δ = −946 ppm, FWHM = 860 Hz) spectra. Crystals of $Bi_8Sn_3Dipp_6$ (**4**) suitable for X-ray crystallography were obtained after removal of the solvent and recrystallization of crude products from *n*-pentane at −30 °C. (Fig. 1) Again, concomitantly formed *cyclo*-$(Dipp_2Sn)_3$ (**5**) was isolated and structurally authenticated. Next to the isolated main products **4** and **5**, also a few octahedral, brownish red single crystals of $Bi_2Sn_4Dipp_6$ (**7**) were found in crude products of the conversion of $Dipp_2SnH_2$ with $Bi[N(SiMe_3)_2]_3$. (Fig. 3) Formation of **1** and **4** from

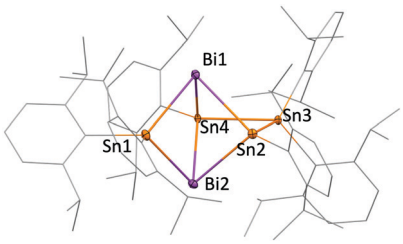

Fig. 3 Molecular structure of **7** in the solid state (50% probability), hydrogens are omitted. For key structural parameters *cf.* Table 1.

cyclotristannanes **2** and **5** *via* reaction with bismuth amide was ruled out experimentally. While keeping the original reaction mixture at *r.t.* for extended times of 6–9 days resulted in complete consumption of **3** and **6** and formation of **1** and **4**, attempts to obtain **1** and **4** by addition of $Bi[N(SiMe_3)_2]_3$ to DME solutions of previously isolated 3 and **6** failed with ArH as the only tractable reaction product. Only when both, Ar_2SnH_2 and $Bi[N(SiMe_3)_2]_3$ were added, consumption of **3** and **6** and formation of **1** and **4** was observed. We hence believe that the formation of labile Bi–H species are crucial steps in Bi–Bi bond formation *en route* to **1** and **4**, where Ar_2SnH_2 acts as the reducing agent for the Bi(0) while being converted into the cyclotristannanes **2** and **5**.

The core structure of **1** and **4** is related to that of Zintl ions of type $[Pn_{11}]^{3-}$ (Pn = P, As, Sb, Bi) and their uncharged derivatives $Pn_{11}R_3$ (Pn = P (R = $SiMe_3$, iPr), As (R = $SiMe_3$)).[41–44] Due to its extraordinary polyhedral arrangement, the long-known $[P_{11}]^{3-}$ has been described as '*ufosan*'-type polyhedral arrangement. Its heaviest congener $[Bi_{11}]^{3-}$ was only recently isolated.[45] In accordance with the principle of valence isoelectronicity, **1** and **4** are topologically identical to $[Bi_{11}]^{3-}$ with each anionic bismuth atom interchanged with an $[Ar_2Sn]$ unit. The arrangement of the Bi atoms in **1** and **4** is also reminiscent of the puckered structure of grey bismuth, where the interlayer distance (3.529 Å) exceeds the Bi–Bi distance of 3.072 Å only by *ca.* 15%. In **1** and **4**, anti-facing Bi_4 tetrahedra are connected by Bi–Bi bonds and Ar_2Sn units. Related structural motifs have been observed for Zintl-ion like intermetalloid clusters of p-block and d-block elements. Yet, examples for solely mixed main group metal clusters are scarce as outlined in a recent review.[46]

All Bi–Bi bond lengths in **1** and **4** (2.9399(6) to 3.0267(6) Å) fall into the known range for Bi–Bi single bonds (Bi_2Ph_4:[47] 2.990 Å, $Bi_2(C_{18}H_{21}N)_2$:[48] 3.0648 Å), and are somewhat shorter than in rhombohedral bismuth (3.072 Å).[49] In agreement with findings in $[Bi_{11}]^{3-}$, average bond distances between apical bismuth atoms (Bi1 and Bi5 in **1**; Bi1 and Bi1$^{\#}$ in **4**) and equatorial atoms (Bi2 to Bi4 and Bi6 to Bi8 in **1**; Bi2, Bi3, Bi4 and equivalents # in **4**) are in average longer than between two equatorial bismuth atoms (**1**: 3.0264(2) *vs.* 2.9476(6) Å; **4**: 3.0047(1) *vs.* 2.9606(4) Å; $[Bi_{11}]^{3-}$:[45] 3.0179(8) *vs.* 2.9621(1) Å). The difference in bond length can be explained by NBO analysis of a model compound $Bi_8Sn_3Ph_6$. The calculations show a higher electron occupation of σ* Bi–Bi bond orbitals of apical bismuth atoms (0.084 e^-) than between equatorial bismuth atoms (0.049 e^-) through electron donation from adjacent σ

Bi–Bi bond orbitals as well as lone pairs of the bismuth atoms into these antibonding orbitals. Angles around apical Bi atoms in **1** (103.47(2) to 105.19(2)°) and **4** (102.74(8) to 105.78(2)°) deviate significantly from the expected 90° value for dominant p character of the bonding orbitals within 2c2e bonds, similar to the angles observed around the tricoordinate Bi atoms in $[Bi_{11}]^{3-}$ (99.58(4) to 108.26(4)°).

The angles around the tin atoms in **1** and **4** are widened (**1**: 105.58(2) to 107.64°; **4**: 106.48 to 107.41(2)°) as compared to the respective Bi–Bi^{-}–Bi angles in $[Bi_{11}]^{3-}$ (94.09(5) to 96.47(4)°). Average Bi–Sn bond distances of $Bi_8Sn_3Ar_6$ (**1**: 2.9162(1) Å, **4**: 2.9060(6) Å) agree with the average Bi–Sn bond value found in the thus far only other structurally characterized, uncharged compound containing a Bi–Sn bond, $Bi_8[Sn(SiMe_3)_3]_6$ (2.926(8) Å).[40] Yet, average Bi–Sn bond distances in **1** and **4** are shorter than in bismuth/tin containing polyhedral polyanions (*e.g.* $[Sn_2Bi_2]^{2-}$: 2.9635(7) Å; $[Sn_3Bi_5]^{3-}$:[26] 2.9975(11) Å). These average bond lengths also exceed average Bi–Sn bonds in **3** (2.9046(8) Å), **6** (2.9084(5) Å), and **7** (2.939(1) Å). Both, **3** and **6**, feature a unique bicyclo[2.2.0]motif with Bi atoms as bridgeheads. The structure can be derived from a hypothetical Bi_4 tetrahedron upon insertion of two tin atoms and substitution by two terminal Ar_2SnH groups. (Fig. 2) Owing to the constrained geometry, the Bi–Bi–Bi angles in **3** and **6** are quite acute at values below 90°. Dihedral angles just below 60° place the Ar_2SnH–substituted Bi atoms in **3** and **6** at intramolecular distances of only 4.028(1) and 3.840(1) Å. A similar distance between Bi atoms of 4.084(1) Å is found in **7**, where a propellane-type structure is extended with a ($Dipp_2Sn$) unit, similar to the purely tin containing compound Sn_6Tripp_6.[50] While Sn–Sn bond lengths in **7** are unremarkable, Bi–Sn bonds (avg. 2.941(2) Å) are elongated compared to **1** and **4** and angles around bismuth in **7** are acute (69.15(4) to 80.72(5)°). Both trends suggest dominant p character of the bonding orbitals of the bismuth atoms in **7** and hence high s character of the lone pairs. The small amount of isolated **7** prevented full spectroscopic characterization thus far. Structural data of the isolated mixed bismuth/tin compounds is summarized in Table 1 and the ESI† (Table S1).

To obtain deeper insight into nature of bonding within the isolated compounds (**1** to **7**), DFT calculations with Gaussian09 program package[51] were performed for phenyl substituted derivatives, $Bi_8Sn_3Ph_6$, $Bi_4Sn_4Ph_8$ and $Bi_2Sn_4Ph_6$, where calculated structures reproduce experimental data. (For full computational details, additional canonical orbitals and structural comparison see ESI†). In all cases, frontier MOs are delocalized over several atoms or the entire metal scaffold as expected for cluster type compounds, *cf.* Fig. 4. While valence MOs for $Bi_8Sn_3Ph_6$ (LUMO+3 to HOMO−10) and $Bi_4Sn_4Ph_8$ (LUMO+3 to HOMO−2) show only minor to no contribution of the aryl ligands, substituents in $Bi_2Sn_4Ph_6$ significantly contribute to calculated canonical orbitals except for the HOMO and LUMO. (see ESI†) Energies for calculated HOMOs of $Bi_8Sn_3Ph_6$ (−5.47 eV), $Bi_4Sn_4Ph_8$ (−5.57 eV) and $Bi_2Sn_4Ph_6$ (−5.36 eV) coincide with each other and are largely composed of s-electron density at bismuth. LUMOs decrease in energy for the extended compounds $Bi_4Sn_4Ph_8$ (−2.17 eV) and $Bi_8Sn_3Ph_6$ (−2.29 eV) as compared to $Bi_2Sn_4Ph_6$ (−1.61 eV) resulting in a decrease of HOMO–LUMO gaps with cluster size ($Bi_2Sn_4Ph_6$: 3.75 eV; $Bi_4Sn_4Ph_8$: 3.39 eV; $Bi_8Sn_3Ph_6$: 3.19 eV). Owing to the spherical shape and similar to results for $[Bi_{11}]^{3-}$, the HOMO in $Bi_8Sn_3Ph_6$ represents a 3d-type superatom orbital, while HOMO−3 is 2p-orbital like. HOMO to HOMO−10 represent Sn and Bi contribution, while HOMO−11 to HOMO−24 are ligand centered. Hence, the 2s-type orbital in $Bi_8Sn_3Ph_6$ ranks lower in energy and corresponds to HOMO−26 as compared to HOMO−10 in the Zintl ion.

Table 1 Bond distances and angles (Bi^a: *apical* Bi atoms, Bi^e: *equatorial* Bi atoms, for **1**, **4** and **7** *cf.* Fig. 1–3)

Distances [Å] and Angles [°]	
1	$[Bi_{11}]^{3-}$
Bi^a–Bi^e: 3.0075(7)–3.0276(6)	Bi^a–Bi^e: 2.996(1)–3.014(2)
Bi^e–Bi^e: 2.9399(6)–2.9559(6)	Bi^e–Bi^e: 2.917(2)–2.998(2)
Bi^e–Sn: 2.9027(9)–2.9433(9)	Bi^e–Bi^a–Bi^e: 100.99(4)–104.69(4)
Bi^e–Bi^a–Bi^e: 103.47(2)–105.19(2)	Bi^a–Bi^e–Bi^e: 99.58(4)–108.26(4)
Bi^a–Bi^e–Bi^e: 103.93(7)–104.90(2)	$Bi^{a/e}$–Bi–$Bi^{a/e}$: 94.09(11)–96.47(4)
Bi^e–Sn–Bi^e: 105.58(2)–107.94(3)	
Sn–Bi^e–$Bi^{a/e}$: 99.97(2)–98.60(2)	
4	**7**
Bi^a–Bi^e: 2.9951(5)–3.0138(5)	Bi1–Bi2: 4.084(3)
Bi^e–Bi^e: 2.9553(7)–2.9714(8)	Sn–Bi: 2.909(1)–2.969(1)
Bi^e–Sn: 2.8966(6)–2.9166(7)	Sn2–Sn4: 3.360(1)
Bi^e–Bi^a–Bi^e: 102.74(8)–105.17(2)	Sn2–Bi1/2–Sn4: 69.13(3)/69.42(3)
Bi^a–Bi^e–Bi^e: 103.85(2)–105.78(2)	Bi1–Sn2/4–Bi2: 87.26(3)/87.49(3)
Bi^e–Sn–Bi^e: 106.48(2)–107.41(2)	Sn2–Sn3–Sn4: 72.84(4)
Sn–Bi^e–$Bi^{a/e}$: 89.05(2)–99.14(2)	

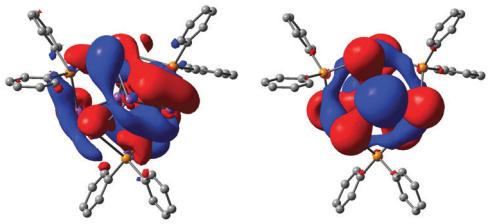

Fig. 4 Lowest unoccupied (left) and highest occupied (right) molecular orbitals of model compounds $Bi_8Sn_3Ph_6$. For full computational details and molecular orbitals of $Bi_4Sn_4H_2Ph_8$ and $Bi_2Sn_4Ph_6$ see ESI.†

In summary, we have isolated the first structurally characterized examples of uncharged Bi/Sn clusters, $Bi_8Sn_3Ar_6$ and $Bi_2Sn_4Ar_6$ utilizing a hydrostannolysis-type reaction of diaryltin dihydrides and a bismuth(III) amide highlighting the synthetic potential of the herein employed synthetic protocol. The concept is currently extended to the preparation of other low-coordinate homo- and heteroatomic main group element compounds. These results will be reported elsewhere.

B. G. S. thanks the Austrian Academy of Sciences for supporting this work with the DOC fellowship. We thank Dr David J. Liptrot for helpful discussion on this project.

Conflicts of interest

There are no conflicts to declare.

Notes and references

1 A. Schnepf, *Chem. Soc. Rev.*, 2007, **36**, 745–758.
2 A. Schnepf, in *Structure and Bonding*, ed. S. Dehnen, Springer, 2017, vol. 119, pp. 135–200.
3 I. Krossing, in *Molecular Clusters of the Main Group Elements*, ed. M. Driess and H. Nöth, Wiley-VCH Verlag GmbH & Co. KGaA, Weinheim, 2005, pp. 209–229.
4 A. F. Richards, H. Hope and P. P. Power, *Angew. Chem., Int. Ed.*, 2003, **42**, 4071–4074.
5 A. F. Richards, M. Brynda and P. P. Power, *Organometallics*, 2004, **23**, 4009–4011.
6 D. Nied, P. Ona-Burgos, W. Klopper and F. Breher, *Organometallics*, 2011, **30**, 1419–1428.
7 A. Jana, V. Huch, M. Repisky, R. J. F. Berger and D. Scheschkewitz, *Angew. Chem., Int. Ed.*, 2014, **53**, 3514–3518.
8 R. J. Wilson and S. Dehnen, *Angew. Chem., Int. Ed.*, 2017, **56**, 3098–3102.
9 M. Dräger and B. Mathiasch, *Angew. Chem.*, 1981, **93**, 1079–1080.
10 M. Driess, S. Martin, K. Merz, V. Pintchouk, H. Pritzkow, H. Grützmacher and M. Kaupp, *Angew. Chem., Int. Ed. Engl.*, 1997, **36**, 1894–1896.
11 M. Westerhausen, M. Krofta, N. Wiberg, J. Knizek, H. Nöth and A. Pfitzner, *Z. Naturforsch., B: J. Chem. Sci.*, 1998, **53**, 1489–1493.
12 F. García, J. P. Hehn, R. A. Kowenicki, M. McPartlin, C. M. Pask, A. Rothenberger, M. L. Stead and D. S. Wright, *Organometallics*, 2006, **25**, 3275–3281.
13 S. Almstätter, M. Eberl, G. Balázs, M. Bodensteiner and M. Scheer, *Z. Anorg. Allg. Chem.*, 2012, **638**, 1739–1745.
14 R. C. Haushalter, B. W. Eichhorn, A. L. Rheingold and S. J. Geib, *Chem. Commun.*, 1988, 1027–1028.
15 S. Traut and C. Von Hänisch, *Z. Anorg. Allg. Chem.*, 2011, **637**, 1777–1783.
16 C. M. Knapp, J. S. Large, N. H. Rees and J. M. Goicoechea, *Dalton Trans.*, 2011, **40**, 735–745.
17 A. Hinz and J. M. Goicoechea, *Dalton Trans.*, 2018, **47**, 8879–8883.
18 R. J. Wilson, B. Weinert and S. Dehnen, *Dalton Trans.*, 2018, **47**, 14861–14869.
19 F. Lips, I. Schellenberg, R. Pöttgen and S. Dehnen, *Chem. – Eur. J.*, 2009, **15**, 12968–12973.
20 M. M. Gillett-Kunnath, A. G. Oliver and S. C. Sevov, *J. Am. Chem. Soc.*, 2011, **133**, 6560–6562.
21 R. J. Wilson, F. Weigend and S. Dehnen, *Angew. Chem., Int. Ed.*, 2020, **59**, 14251–14255.
22 S. C. Critchlow and J. D. Corbett, *Inorg. Chem.*, 1982, **21**, 3286–3290.
23 F. Lips and S. Dehnen, *Angew. Chem., Int. Ed.*, 2009, **48**, 6435–6438.
24 F. Lips, M. Raupach, W. Massa and S. Dehnen, *Z. Anorg. Allg. Chem.*, 2011, **637**, 859–863.
25 U. Friedrich, M. Neumeier, C. Koch and N. Korber, *Chem. Commun.*, 2012, **48**, 10544–10546.
26 U. Friedrich and N. Korber, *ChemistryOpen*, 2016, **5**, 306–310.
27 K. Mayer, J. V. Dums, W. Klein and T. F. Fässler, *Angew. Chem., Int. Ed.*, 2017, **56**, 15159–15163.
28 F. Lips, M. Hołyńska, R. Clérac, U. Linne, I. Schellenberg, R. Pöttgen, F. Weigend and S. Dehnen, *J. Am. Chem. Soc.*, 2012, **134**, 1181–1191.
29 M. M. Gillett-Kunnath, A. Muñoz-Castro and S. C. Sevov, *Chem. Commun.*, 2012, **48**, 3524–3526.
30 F. Pan, L. Guggolz, F. Weigend and S. Dehnen, *Angew. Chem., Int. Ed.*, 2020, **59**, 16638–16643.
31 S. Heiles, R. L. Johnston and R. Schäfer, *J. Phys. Chem. A*, 2012, **116**, 7756–7764.
32 S. Heiles, K. Hofmann, R. L. Johnston and R. Schäfer, *ChemPlusChem*, 2012, **77**, 532–535.
33 P. R. Sharp and M. T. Rankin, *Inorg. Chem.*, 1986, **25**, 1508–1510.
34 E. Subashi, A. L. Rheingold and C. S. Weinert, *Organometallics*, 2006, **25**, 3211–3219.
35 S. Harrypersad and D. Foucher, *Chem. Commun.*, 2015, **51**, 7120–7123.
36 S. Masamune and L. R. Sita, *J. Am. Chem. Soc.*, 1985, **107**, 6390–6391.
37 F. J. Brady, C. J. Cardin, D. J. Cardin, M. A. Convery, M. M. Devereux and G. A. Lawless, *J. Organomet. Chem.*, 1991, **421**, 199–203.
38 H. Schumann and M. Schmidt, *Angew. Chem.*, 1964, **76**, 344.
39 G. Becker and M. Rößler, *Z. Naturforsch., B: Anorg. Chem., Org. Chem.*, 1982, **37**, 91–96.
40 G. Linti and W. Köstler, *Z. Anorg. Allg. Chem.*, 2002, **628**, 63–66.
41 W. Wichelhaus and H. G. Von Schnering, *Naturwissenschaften*, 1973, **60**, 104.
42 H. G. Schnering, D. Fenske, W. Hönle, M. Binnewies and K. Peters, *Angew. Chem., Int. Ed. Engl.*, 1979, **18**, 679–680.
43 K.-F. Tebbe, *Z. Anorg. Allg. Chem.*, 1989, **572**, 115–125.
44 T. Hanauer and N. Korber, *Z. Anorg. Allg. Chem.*, 2006, **632**, 1135–1140.
45 B. Weinert, A. R. Eulenstein, R. Ababei and S. Dehnen, *Angew. Chem., Int. Ed.*, 2014, **53**, 4704–4708.
46 R. J. Wilson, N. Lichtenberger, B. Weinert and S. Dehnen, *Chem. Rev.*, 2019, **119**, 8506–8554.
47 F. Calderazzo, A. Morvillo, G. Pelizzi and R. Poli, *Chem. Commun.*, 1983, 507–508.
48 S. Shimada, J. Maruyama, Y. K. Choe and T. Yamashita, *Chem. Commun.*, 2009, 6168–6170.
49 A. F. Holleman, N. E. Wiberg and G. Fischer, *Lehrbuch der Anorganischen Chemie*, Walter de Gruyter, Berlin New York, 2007.
50 C. P. Sindlinger and L. Wesemann, *Chem. Sci.*, 2014, **5**, 2739–2746.
51 M. J. Frisch, G. W. Trucks and H. B. Schlegel, *et al.Gaussian 09, (Revision D.01)*, Gaussian, Inc., Wallingford, CT, 2013.

